Mechanism and characterization of nanosecond laser rust-removal on AH36 steel*

TAO Qing[1,2], KUANG Wenxiang[1], WEI Liangpeng[1], YIN Yegang[1], CHENG Jian[1], and LIU Dun[1]**

1. Laser Group, School of Mechanical Engineering, Hubei University of Technology, Wuhan 430068, China

2. Hubei Key Laboratory of Modern Manufacturing Quantity Engineering, School of Mechanical Engineering, Hubei University of Technology, Wuhan 430068, China

(Received 3 August 2022; Revised 27 October 2022)

In this paper, the effects of different laser powers, repetition rates, and spot overlaps on the surface roughness, micromorphology, and Vickers hardness of rusted AH36 steel were researched in the rust removal experiment of fiber pulse laser on the marine steel surface. Then, the mechanical properties, corrosion resistance, and metallographic microstructure of the surface of samples after laser cleaning were analyzed. The experimental results show that when the processing parameters were the laser power of 40 W, the repetition rate of 110 kHz, and the spot overlap of 50%, the rust removal effect on AH36 steel was the best, and it met the cleanliness standard of marine steel coating. Moreover, its Vickers hardness, mechanical properties, corrosion resistance, and repainting properties were superior to those of the original substrate.

Document code: A **Article ID:** 1673-1905(2023)04-0227-8

DOI https://doi.org/10.1007/s11801-023-2136-8

Due to the long-term working of marine ships in the harsh environment at sea, they were prone to rust, which seriously threatened their safety. Therefore, it was necessary to regularly remove rust on the surface of ships[1]. The traditional rust removal methods could be divided into three types, sandpaper polishing, sandblasting, and chemical rust removal. Among them, sandpaper grinding and rust removal were done manually, which were low-efficiency. Sandblasting was easy to damage the substrate surface. The standard chemical rust removal was acid pickling, and its cleaning efficiency was low[2,3]. Because laser cleaning technology had no pollution, non-contact and no damage to the substrate, many scholars focused on this field[4,5].

Laser cleaning technology was first used to remove dirt from artwork[6], and later the technology was optimized and gradually applied to various metal materials. LI et al[7] used a nanosecond laser to clean 30-μm-thick Al-Si coating on boron steel. The experimental results showed that the ablation depth gradually increased until it reached a constant value. LI et al[8] cleaned the painted marine steel surface with an Nd: YAG pulsed laser, and after cleaning, the surface roughness ranged from 2.048 μm to 2.570 μm. After repainting, the adhesion strengths of the surfaces with *Ra* of 2.253 μm and 2.048 μm were 20 MPa and 7.6 MPa, respectively, which were higher than the standard adhesion strength of marine materials by 3 MPa. ZHOU et al[9] used nanosecond lasers to explore the rust removal mechanism of AH32 marine steel, and they finally found that the main mechanisms are blasting and evaporation. LI et al[10] used a fiber laser with a wavelength of 1 064 nm to remove the rust layer on the surface of Q345 steel. After laser cleaning, the electrochemical corrosion property was improved. QIAO et al[11] studied the descaling process of 45-gauge carbon steel using a YAG pulsed laser with a wavelength of 1 064 nm. The elemental content of the sample surface after laser cleaning was analyzed. The results showed that the laser did not cause other chemical reactions on the surface of the carbon steel. Most existing literature was about common steel, but marine high-strength steel was not researched enough. AH36 steel was low-alloy shell steel with high strength and good seawater corrosion resistance. Currently, the application of laser rust removal technology in marine engineering still needed improvement.

In this paper, a nanosecond pulse laser with a wavelength of 1 064 nm was used to clean the rusted surface of AH36 steel. The sample's surface roughness, micromorphology, Vickers hardness, mechanical properties, corrosion resistance, and metallographic structure were analyzed by changing the laser power, repetition rate, and spot overlap, and so on. It could effectively prolong the service life of marine steel.

* This work has been supported by the Natural Science Foundation of Hubei Province (No.2017CFB685), Hubei University of Technology "Advanced Manufacturing Technology and Equipment" Collaborative Innovation Center Open Research Fund (Nos.038/1201501 and 038/1201803), and the College-Level Project of Hubei University of Technology (No.4201/01758).

** E-mail: dun.liu@hbut.edu.cn

The experimental system was shown in Fig.1. The pulsed fiber laser had a central wavelength of 1 064 nm, a laser power range of 10—60 W, a pulse width of 10—240 ns, a spot diameter of 42 μm, and a repetition rate of 70—1 000 kHz.

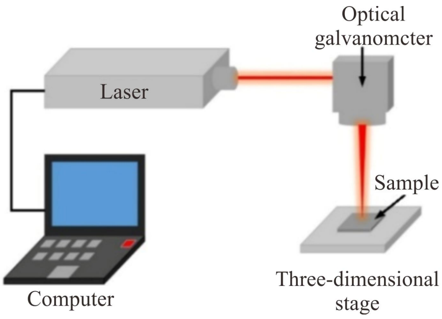

Fig.1 Experimental system

The sample was AH36 steel. The dimensions of the original sample were 80 mm×80 mm×5 mm, as shown in Fig.2(a). Then, the surface of the samples was sprayed and wetted with 3%—4% NaCl solution every 12 h in a humid environment for a corrosion time of two months. The rust grade of the samples was B[12] as shown in Fig.2(b).

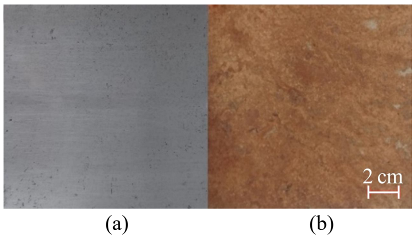

Fig.2 The samples: (a) Original sample; (b) Rust sample

Factors that affected the cleaning effect included laser power, scanning speed (V)[13], spot diameter (D), and spot overlap distance (L)[14] in Fig.3.

Single factor experiments were used to research the rust layer's surface roughness, Vickers hardness, and removal efficiency. The cleaning effect was evaluated by the surface roughness, micro-morphology or macro-morphology. The optimal laser-cleaning parameters were obtained through cross experiments. Then, the samples cleaned by laser and hands were compared for mechanical properties, corrosion properties, metallographic structure, and repaint performance.

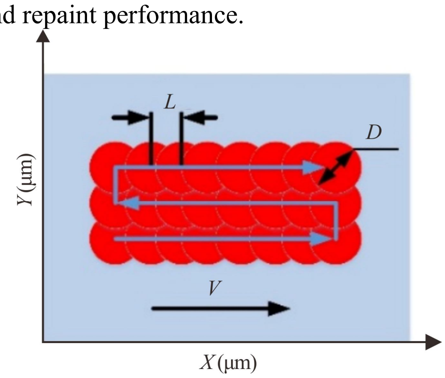

Fig.3 Spot scanning path

Vickers hardness tester and Bruker surface profilometer were used to obtain the hardness and surface roughness of the sample, respectively. The microscopic morphology of the cleaned sample was observed by the Nikon microscope and scanning electron microscope (SEM). Mechanical properties and metallographic organization of the cleaned sample were analyzed through the microcomputer-controlled electronic universal material testing machine and metallographic microscope. The repainting performance of the cleaned sample was obtained through cross-cut-tester[15].

The laser power was ranged from 10 W to 60 W, the laser overlap rate was 50%, and the repetition rate was 110 kHz. As shown in Fig.4, when laser power increased continuously, the rust layer began to fall off. While laser power was 30 W, the sample started to expose some original metal substrate. However, there was still some rust attached to sample's surface. When laser power became 40 W, rust layer was almost removed and all metal substrate was shown. As laser power was more than 50 W, sample's surface became pale-yellow. Because the substrate was oxidized again to form a new oxide layer, the optimal laser power was 40 W.

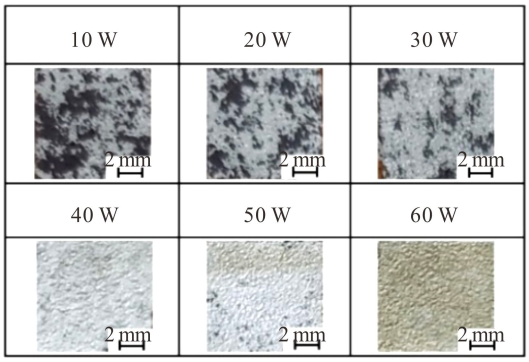

Fig.4 Cleaning effect with different laser powers

The repetition rate was in the range of 80—130 kHz, the laser overlap rate was 50%, and laser power was 40 W. As shown in Fig.5, with the increase of repetition rate, single pulse energy decreased, and the number of pulses increased so that the laser cleaning effect was more obvious. When the repetition rate was of 80—100 kHz, pulse energy ablating on the sample's surface was large. The rust layer was removed, and the substrate was oxidized to be pale yellow. While the repetition rate was 120—130 kHz, pulse energy acting on the surface of the sample was relatively low. And there was some residual rust on the surface, which made the cleaning effect bad. So when the repetition rate was 110 kHz, the laser cleaning effect was the best.

The spot overlap was in the range of 20%—70%, the repetition rate was 110 kHz, and laser power was 40 W in Fig.6. When the laser spot overlap was low, the cleaning effect was not good. Until the spot overlap reached 50%, the sample surface showed the best cleaning effect.

When the spot overlap was greater than 60%, the surface of the sample was light yellow. Some pits and new oxide layers appeared on the microscopic morphology. Therefore, 50% spot overlap was the best.

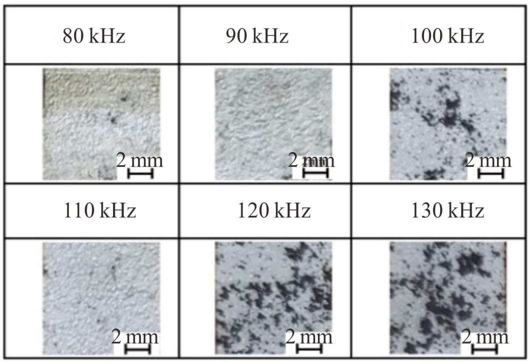

Fig.5 Cleaning effect with different repetition rates

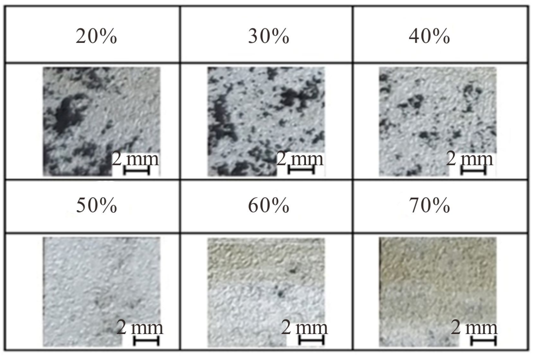

Fig.6 Cleaning effect with different spot overlaps

The effects of different laser powers on the surface roughness of samples were explored. With the increase of laser power, the surface temperature of rusted layer increased, and more rust melted and gradually fell off in Fig.7(a) and (b). When laser power was 40 W, the surface roughness gradually decreased to reach a minimum value of 2.12 μm, which was lower than the original surface roughness of 4.25 μm in Fig.8(a). The fluidity of fused slurry increased with the increase of pulsed laser pressure, the fused slurry spread around, which made the surface roughness slightly increase.

Obviously, the surface roughness decreased with the increasement of repetition rate in Fig.8(b). When the repetition rate was 110 kHz, the surface roughness was the lowest, which was 2.24 μm in Fig.9(d). As the repetition rate increased in the range of 80—110 kHz, the residue of rust layer decreased and the cleaning effect was good. When repetition rate increased in the range of 110—130 kHz, the energy of single pulse decreased, so the residue of rust layer slightly increased, and the surface roughness increased slightly in Fig.7(e).

When the spot overlap was lower, the surface roughness of sample was higher in Fig.8(c). As the spot overlap increased in the range of 20%—50%, the surface roughness of sample decreased. While the spot overlap was 50%, surface roughness decreased to a minimum of 2.20 μm in Fig.7(g). At this time, the absorption energy of rust layer increased. The ability of rust to melt, evaporation, and peeling was improved, and the surface roughness decreased, so the residual rust layer gradually reduced. When the spot overlap was in the range of 50%—70%, the scanning speed was slower. With the increase of cleaning time per unit area, the substrate was heated again and appeared molten state in Fig.7(h), which caused the surface roughness to increase again.

Finally, the optimal laser-cleaning parameters were obtained as follows, laser power of 40 W, repetition rate of 110 kHz, and spot overlap of 50%.

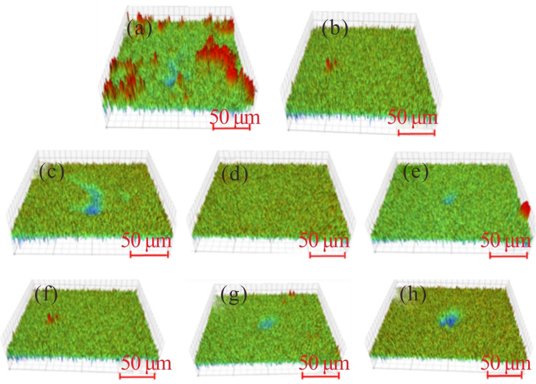

Fig.7 3D morphology of samples after laser cleaning: (a) 10 W; (b) 40 W; (c) 80 kHz; (d) 110 kHz; (e) 130 kHz; (f) 30%; (g) 50%; (h) 70%

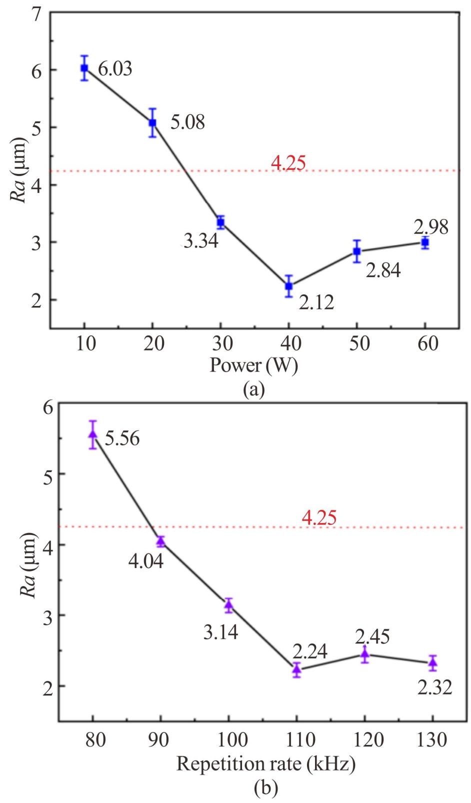

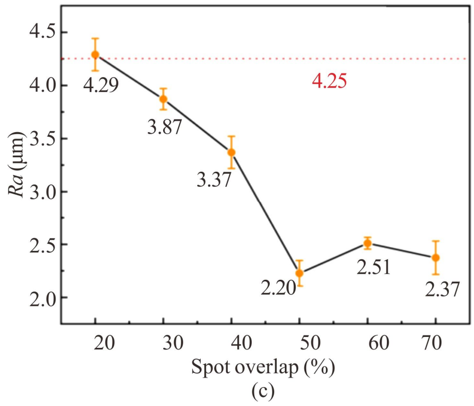

Fig.8 Surface roughness curves of samples after laser cleaning under different parameters: (a) Laser powers; (b) Repetition rates; (c) Spot overlap

The surface micro-morphology of sample after laser cleaning was tested by transflective polarizing microscope with different laser powers, repetition rates, and spot overlaps. The experimental results were shown in Fig.9. When laser power was 10 W, there was still some rust on the surface of sample due to lower laser energy in Fig.9(a). With the increase of laser power, the rust on the surface of sample was gradually removed. When laser power reached 40 W, obviously, there was no rust residue. Because the laser cleaned on the sample's surface, a solid-liquid-solid phase transformation occurred, and a slight ablation and melted traces were found. When laser power became 60 W, the excessive laser energy resulted in some ablated holes on the sample's surface, and the surface was seriously yellow. The single-pulse energy was inversely proportional to the repetition rate in Fig.9(b). The single-pulse power decreased with the increase of pulse repetition rate. When the repetition rate was 80 kHz with the higher single pulse energy, the sample's surface was yellowed, some pits appeared, and the ablation phenomenon was severe. While the repetition rate was 110 kHz, the cleaning effect was the best. As the repetition rate was 130 kHz, the single pulse energy was lower, the cleaning effect was bad, and a large amount of rust remained on the sample's surface. The spot overlap significantly affected the cleaning effect in Fig.9(c). When the spot overlap was 30%, there was still some rust on the sample's surface. The cleaning effect was more evident with the increase of spot overlap. As it reached 50%, there was no rust on the surface. While the spot overlap became 70%, the speed of laser cleaning became slower. Cleaning time per unit area increased so that the substrate was ablated again, and the surface of substrate was oxidized, which was seriously yellowed and damaged, and it had a bad cleaning effect. When laser power was 40 W, the repetition rate was 110 kHz, and the spot overlap was 50%, the minimal surface roughness could be obtained. These parameters were optimal for the best cleaning effect from the microscopic morphology.

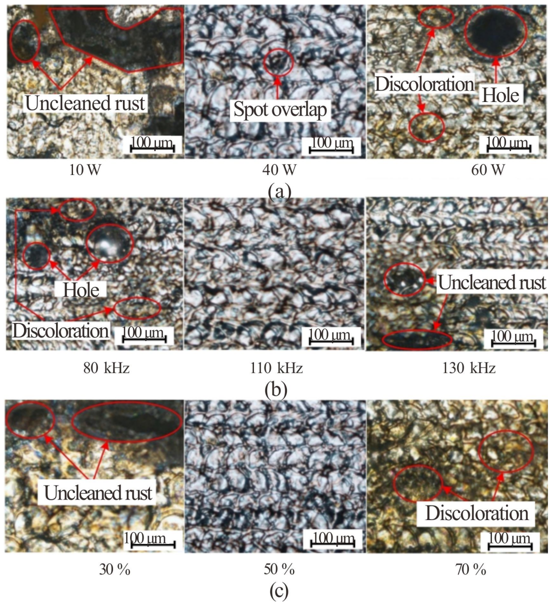

Fig.9 Surface micro-morphology: (a) Laser powers; (b) Repetition rate; (c) Spot overlap

The SEM was used to further explore the influence of laser parameters on the sample. When the repetition rate was 110 kHz, the spot overlap was 50%, and the laser power changed, the obtained microstructures were deeply analyzed.

The uncleaned surface of sample was in Fig.10(a), and there were some rust and rust oxides. The SEM image of polished sample surface by hands was in Fig.10(b). Although the rust was removed, the surface was left with scratches and cracks. It damaged the substrate. The SEM image of cleaned sample surface by laser was in Fig.10(c), whose power was 10 W, the surface was not completely cleaned, so surface microstructure was close to uncleaned sample's one. The SEM image of cleaned sample surface by laser whose power was 40 W was in Fig.10(d). The rust was removed, and the sample's surface had a solid-liquid-solid phase transition, which left slight ablation, and the cleaning effect was the best. The SEM image of cleaned sample surface by laser whose power was 60 W was in Fig.10(e), and there was apparent irregularity. In the process of laser cleaning, some ablation pits formed, and there were melting splashes on the edges of ablation pits, so the surface microstructure was bad.

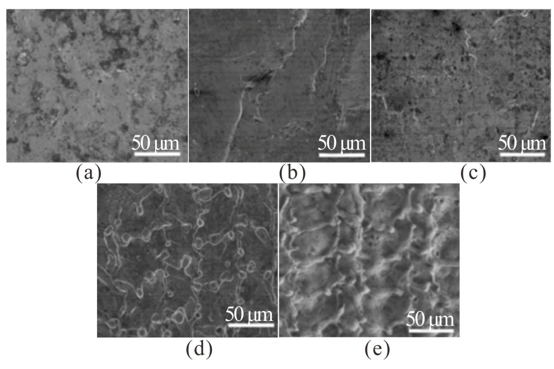

Fig.10 Surface microstructures of samples by SEM

With the increase of laser power, the Vickers hardness of sample surface also increased, and all of them were greater than the one of original substrate, which was 215 HV. While the laser power was 60 W in Fig.11(a), the maximum Vickers hardness reached 232 HV. When the high-energy laser cleaned the sample, its surface was rapidly heated and melted. As it quickly cooled and recrystallized, the surface formed a dense hardened layer, which increased the Vickers hardness of sample. The repetition rate greatly influenced the Vickers hardness of sample in Fig.11(b). When the repetition rate increased, the Vickers hardness of sample also increased, and the maximum Vickers hardness was 236 HV at 110 kHz. Then, it decreased to 229 HV at 130 kHz. When other parameters were constant and repetition rate increased, the number of pulses ablating the sample surface per unit time increased. Therefore, the surface of sample was pressed, which increased the surface strength and generated a dense hardened layer, and Vickers hardness increased. As the pulse repetition rate was more than 120 kHz, Vickers hardness decreased slightly. The laser beam with a high repetition rate ablated on the sample's surface, pulses generated a reverse impact force, which destroyed the hardened layer, and the substrate was oxidized again. While the spot overlap increased, the Vickers hardness of sample also increased in Fig.11(c). The scanning speed was higher, the spot overlap was lower, the time of laser-cleaning was shorter, and the absorbed heat was less by the sample's surface. Therefore, with the increase of spot overlap, the absorbed heat on the sample's surface increased, and the surface crystal grains were denser, so Vickers hardness was greater.

The analysis results of the main elements on the surface of three samples were obtained through energy dispersive spectrometer (EDS) detection in Tab.1 and Fig.12. It could be seen from Tab.1 that the iron and manganese oxides formed after the samples were rusted to reduce the content of iron and manganese, while the contents of carbon and oxygen increased sharply. After the surface of the sample was cleaned by laser, the rust was removed, and the carbon and oxygen elements on the surface of the substrate and the oxygen in the air formed carbon oxides, so these two elements were relatively reduced. Meanwhile, only a small amount of iron and manganese was combined with oxygen. Therefore, compared with the measuring results of original sample, the contents of iron and carbon elements in the measuring results of substrate surface after laser cleaning were slightly increased, while the contents of carbon and oxygen elements were slightly reduced. The effect of the change in oxygen content on corrosion resistance could not be ignored. An increase in oxygen content decreased the corrosion resistance of alloy steels, where the formation of inclusions and an increase in the gap between the inclusions and the substrate were responsible for the corrosion pits. The oxygen content after laser rust removal was lower than that of other samples. In summary, the surface properties of the laser-treated sample were better than those of other samples.

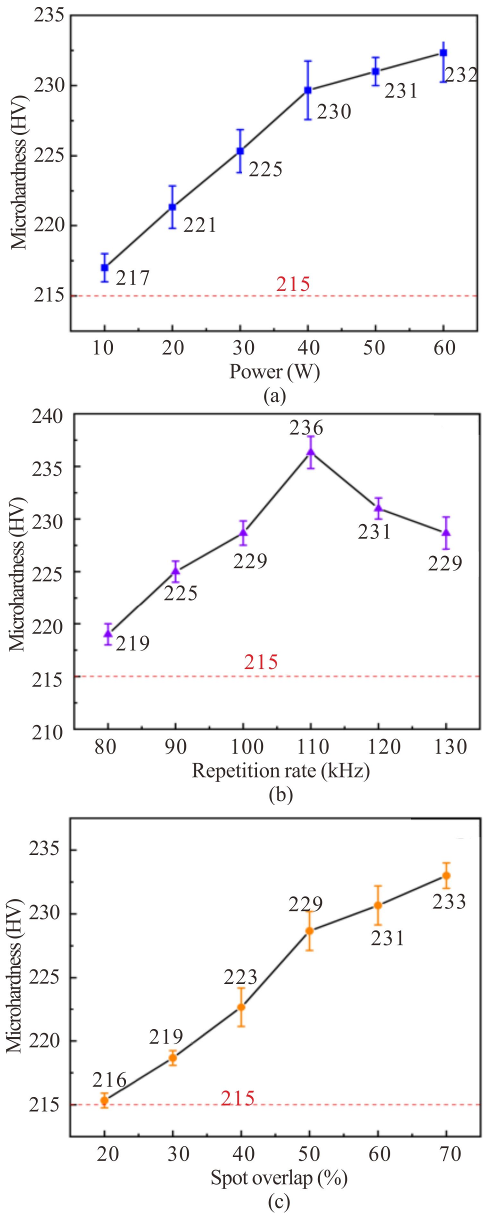

Fig.11 Vickers hardness curves under different laser parameters: (a) Laser powers; (b) Repetition rates; (c) Spot overlaps

Tab.1 Surface elemental contents of different samples

Sample	Fe (wt%)	C (wt%)	O (wt%)	Mn (wt%)
Original	95.60	2.15	0.63	1.62
Rust	55.56	15.98	27.01	1.45
Laser rust removal	96.67	1.04	0.23	2.06

The surfaces of laser-cleaned sample were executed corrosion resistance test, whose results were compared with the hand-polished one, and the test results were shown in Tabs.2—4. The ratio of corrosive agent was 1% salt and 99% di-stilled water. The laser-cleaned surface was immersed in the corrosive agent for 120 h at room temperature. After weighting, the original weight was 19.061 g, the weight after corrosion was 19.038 g, the lost weight was 23 mg, and the average corrosion rate was 0.192. The laser power was higher, and the corrosion resistance of samples was better in Tab.2. When the repetition rate increased, the corrosion resistance of samples increased first and then decreased slightly in Tab.3. As the spot overlap increased, the samples' corrosion resistance increased first and then decreased slightly in Tab.4. After laser cleaning, a re-melted layer was formed on the sample's surface. The re-melted layer was a dense oxide layer, which could improve the corrosion resistance of sample's surface.

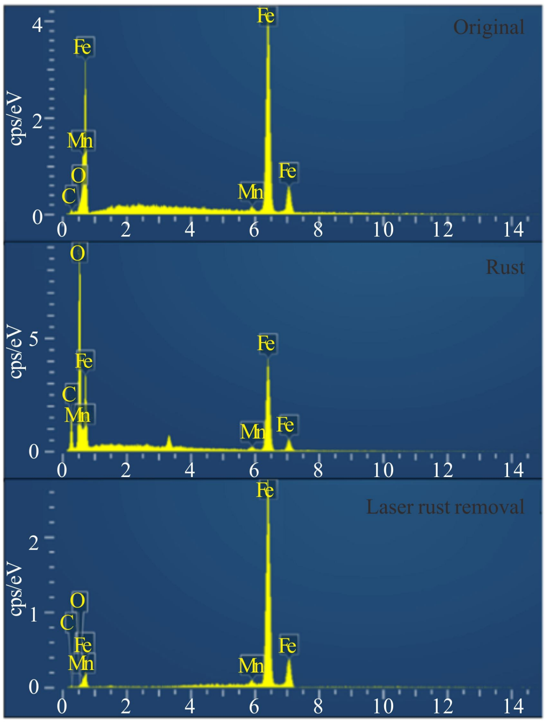

Fig.12 Surface elemental contents of different samples

The corrosion resistance of sample's surface by hand-polishing was lower, and the reasons were as follows. The scratches of substrate's surface caused by hand-polishing were serious, which reduced its corrosion resistance. The laser-cleaned sample only removed the rust layer, while the sample polished by sandpaper increased the surface area of substrate, which made corrode easier. So, laser cleaning could improve the sample's corrosion resistance.

The tensile test was carried out by the CTM9200 electronic universal material testing machine, which referred to the national standard GB/T 228.1-2010. The tensile speed was 2 mm/min, and the stress-strain curve was obtained in Fig.13.

The maximum load and tensile strength of sample after laser cleaning were slightly increased compared with the original sample. Moreover, the maximum load and tensile strength of sample by hand polishing decreased slightly. Because laser heating source was stable, the surface of substrate was uniformly heated. The substrate's mechanical properties were also improved while the rust oxide on the surface of substrate was removed. Due to the uneven force by hand-polishing, this resulted in irregular rust removal. Stress concentrations were generated at the sample's edges, which slightly reduced samples' maximum load and tensile strength. Therefore, laser cleaning technology could remove the rust layer on the surface of sample and improve the mechanical properties of AH36 steel.

The surface of sample cleaned with optimal laser parameters was observed by metallographic microscope to further research the effect of pulsed laser on the substrate while removing rust. The experimental results were shown in Fig.14. The microstructure of sample mainly included ferrite and pearlite. After laser cleaning, the metallographic structure of sample surface was changed. Due to laser heating effect, many lath-like martensite structures were observed in the metallographic structure. With the reduction of crystal grain spacing between the structures, the boundaries of crystal grain increased, which increased the Vickers hardness after laser cleaning[16].

Tab.2 Effect of laser power on corrosion performance

Laser power (W)	Original weight (g)	Weight after corrosion (g)	Lost weight (mg)	Average corrosion rate ($mg/cm^2 \cdot h$)
10	19.869 0	19.850 8	18.2	0.152
40	19.655 0	19.638 4	16.6	0.138
60	19.425 5	19.410 3	15.2	0.127

Tab.3 Effect of repetition rate on corrosion performance

Repetition rate (kHz)	Original weight (g)	Weight after corrosion (g)	Lost weight (mg)	Average corrosion rate ($mg/cm^2 \cdot h$)
90	19.582 1	19.566 1	19.6	0.163
110	18.905 0	18.888 2	16.8	0.140
130	18.565 8	18.545 7	18.4	0.153

Tab.4 Effect of spot overlap on corrosion performance

Spot overlap (%)	Original weight (g)	Weight after corrosion (g)	Lost weight (mg)	Average corrosion rate ($mg/cm^2 \cdot h$)
30	18.605 6	18.587 4	18.2	0.152
50	19.633 0	19.616 8	16.2	0.133
70	19.069 4	19.051 6	17.8	0.148

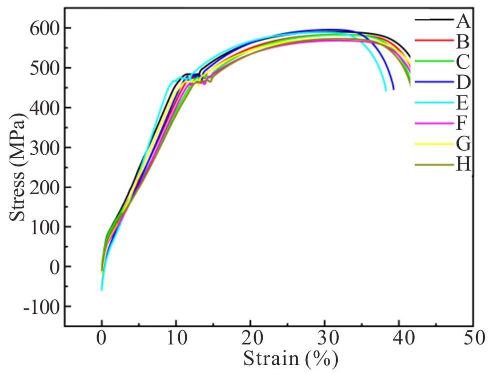

Fig.13 Tensile properties of samples: (a) Original sample; (b) Hand polished; (c) Power (40 W); (d) Power (60 W); (e) Repetition rate (110 kHz); (f) Repetition rate (130 kHz); (g) Spot overlap (50%); (h) Spot overlap (70%)

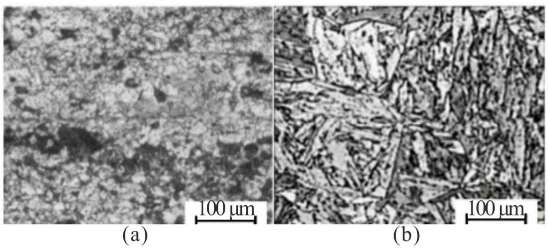

Fig.14 Metallographic micrographs: (a) Original sample; (b) Laser cleaning

The paint was ordinary white paint, and its adhesion standard could be divided into six grades[17]. A cross-cut-tester was used to draw an 8×8 square matrix on the paint layer, then the paint adhesion test was carried out with a special adhesive tape. The sample surface without laser cleaning had a little paint layer, and the experimental results showed its adhesion was grade 1 in Fig.15(a). However, the surface of sample after laser cleaning had entire paint layer, and the edge of incision was smooth, and its adhesion was grade 0 in Fig.15(b). The experimental results showed that the repainting performance of sample after laser cleaning was improved and it was better than that of the original sample.

In this paper, the effects of laser power, repetition rate and spot overlap on the rust layer were investigated in the laser cleaning experiments of AH36 steel. The hardness, corrosion resistance, mechanical properties and recoating performance of the laser cleaned samples were observed and the conclusions were summarized as follows. The optimal parameters for laser cleaning were laser power of 40 W, repetition rate of 110 kHz and

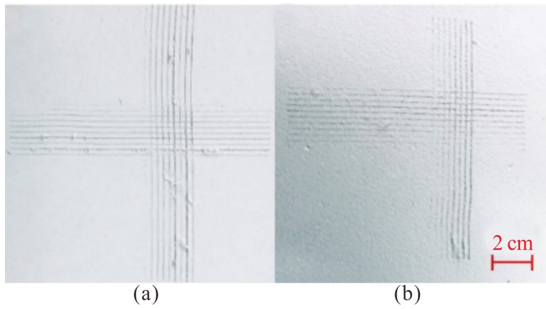

Fig.15 Comparison of repainting performance: (a) Original sample; (b) Laser cleaning

spot overlap of 50%. The hardness, corrosion resistance, mechanical properties and recoating performance of the laser cleaned samples were better than those of original samples.

Statements and Declarations

The authors declared that there were no conflicts of interest related to this article.

References

[1] TIAN Y, ZHANG G, MORIMOTO K, et al. Automated rust removal: rust detection and visual servo control[J]. Automation in construction, 2022, 134: 104043.

[2] CHOUDHURY M D, DAS S, BANPURKAR A G, et al. Regression analysis of wetting characteristics for different random surface roughness of polydimethylsiloxane using sandpapers[J]. Colloids and surfaces A: physicochemical and engineering aspects, 2022, 647: 129038.

[3] YABE A, OKADA M, HARA E S, et al. Self-adhering implantable device of titanium: enhanced soft-tissue adhesion by sandblast pretreatment[J]. Colloids and surfaces B: biointerfaces, 2022, 211: 112283.

[4] LU Y, DING Y, WANG G, et al. Ultraviolet laser cleaning and surface characterization of AH36 steel for rust removal[J]. Journal of laser applications, 2020, 32(3): 032023.

[5] NARAYANAN V, SINGH R K, MARLA D. Laser cleaning for rust removal on mild steel: an experimental study on surface characteristics[J]. MATEC web of conferences, 2018, 221: 01007.

[6] SIANO S, SALIMBENI R. Advances in laser cleaning of artwork and objects of historical interest: the optimized pulse duration approach[J]. Accounts of chemical research, 2010, 43(6): 739-750.

[7] LI F, CHEN X, LIN W, et al. Nanosecond laser ablation of Al-Si coating on boron steel[J]. Surface and coatings technology, 2017, 319: 129-135.

[8] LI X, HUANG T, CHONG A W, et al. Laser cleaning of steel structure surface for paint removal and repaint adhesion[J]. Opto-electronic engineering, 2017, 44(3)：340-344.

[9] ZHOU J Z, LI H T, SUN Q, et al. Laser derusting mechanism of AH32 steel based on cleaned surface topography[J]. Optics and precision engineering, 2019, 27(8)：1754-1764.

[10] LI X Y, LI C Y, WANG D. Effect of laser scanning speeds on cleaning quality of rusted layer on Q345 steel surface[J]. Chinese journal of lasers, 2020, 47(10)：1002010.

[11] QIAO Y L, ZHAO J X, WANG S J, et al. Laser cleaning and elemental composition analysis of rusty surface[J]. Laser & infrared, 2018, 48(3)：299-304.

[12] XU J, GUI C, HAN Q. Recognition of rust grade and rust ratio of steel structures based on ensembled convolutional neural network[J]. Computer-aided civil and infrastructure engineering, 2020, 35(10)：1160-1174.

[13] WAN H, MIN J, LIN J, et al. Effect of laser spot overlap ratio on surface characteristics and adhesive bonding strength of an Al alloy processed by nanosecond pulsed laser[J]. Journal of manufacturing processes, 2021, 62：555-565.

[14] LIN Q, FAN Z J, WANG W, et al. The effect of spot overlap ratio on femtosecond laser planarization processing of SiC ceramics[J]. Optics & laser technology, 2020, 129：106270.

[15] VATER J M, GRUBER F, GRAHLERT W, et al. Prediction of coating adhesion on laser-cleaned metal surfaces of battery cells using hyperspectral imaging and machine learning[J]. Coatings, 2021, 11(11)：1388.

[16] ZHU L X, SUN B T, LI Z, et al. The weld quality improvement via laser cleaning pre-treatment for laser butt welding of the HSLA steel plates[J]. Welding in the world, 2020, 139：106785.

[17] YANG L, SONG H L, CHANG J W. Comparison and analysis of coating cross-cut test in different standards[J]. Coating and protection, 2021, 42(1)：39-42.